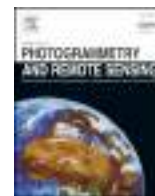




Contents lists available at ScienceDirect

## ISPRS Journal of Photogrammetry and Remote Sensing

journal homepage: [www.elsevier.com/locate/isprsjprs](http://www.elsevier.com/locate/isprsjprs)

## Remote sensing of albedo-reducing snow algae and impurities in the Maritime Antarctica



Pirjo Huovinen<sup>a,b,\*</sup>, Jaime Ramírez<sup>a</sup>, Iván Gómez<sup>a,b</sup>

<sup>a</sup> Instituto de Ciencias Marinas y Limnológicas, Facultad de Ciencias, Universidad Austral de Chile, Valdivia, Chile

<sup>b</sup> Centro FONDAF de Investigación en Dinámica de Ecosistemas Marinos de Altas Latitudes (IDEAL), Valdivia, Chile

### ARTICLE INFO

#### Keywords:

Albedo  
Antarctica  
Light-absorbing impurities  
Sentinel-2A  
Snow algae  
Spectral mixture analysis

### ABSTRACT

Snow algae have been proposed to play a key role in climate change as they can reduce albedo (“bioalbedo”) and thus accelerate the melting of snow and ice fields. Although satellite-derived data has opened opportunities for larger scale observations, remote sensing of snow algae has been scarce and is methodologically challenging due to the presence of other light-absorbing impurities (LAIs). So far the studies on the role of LAIs in reducing albedo and increasing melting have been strongly focused on the Arctic ice sheets. The aims of the present study were to compare the relative impact of microalgae and other LAIs in reducing albedo in the snow of Fildes Peninsula, King George Island, Maritime Antarctica, using Spectral Mixture Analysis (SMA), which allows mapping sub-pixel fractions of multiple components in mixed pixels from satellite-derived data (Sentinel-2A). Also, the applicability of band ratios previously proposed for classifying snow algae (Red-Green band ratio) and impurities (Snow Darkening Index (SDI)) was tested and compared with SMA. Ground validation was made by characterizing the composition of snow algae (through chlorophyll *a* fluorescence) and by measurements of spectral absorption of solar radiation in red and green snow. SMA resulted a reliable method to classify snow algae and impurities with low amount of false positives (user accuracy 92–93%). However, omission error derived from dominant type (> 50% abundance) confusion matrix was higher (producer accuracy for algae 63% and impurity 53%). In contrast, classification with band ratios resulted in large number of false positives (user accuracy for SDI 36%, for R/G 46%), and even higher omission error for R/G (producer accuracy 36%), whereas SDI had better producer accuracy (68%). SMA provided higher precision in separating dominant LAIs than the band ratios, which resulted in widely overlapping signals. Reduced albedo could be related with SMA-derived snow algae and impurity abundancies at albedo levels > 45% for algae and > 30% for impurities.

### 1. Introduction

Snow has a key role in the earth’s energy balance, pure fresh snow generally presenting high albedo in near-UV and visible wavelengths (80–90%; Wiscombe and Warren, 1980; Dozier and Painter, 2004), decreasing in older, wet snow (around 50–60%; Thomas and Duval, 1995). In addition to an increased grain size in aging snow, light-absorbing impurities (e.g. soot, dust, black carbon, cryoconite) can also reduce albedo and thus the melting of snow and ice fields (Warren and Wiscombe, 1980; Cook et al., 2016). Actually, faster melting rates of glaciers than those estimated by current models are proposed to take place due to this phenomenon (Tedesco et al., 2016). Recently, darkening of snow (“dark snow”) in the Arctic has received both scientific and media attention, and has been linked with the massive loss of ice sheets in Greenland in 2012 (Benning et al., 2014; Dumont et al., 2014;

Shimada et al., 2016; Tedesco et al., 2015, 2016, 2017). In the Antarctic, the Antarctic Peninsula is the area that has experienced the most rapid regional warming during the last decades (Vaughan et al., 2001, 2003; Clarke et al., 2012), and retreat of glacier fronts have been reported here as well as in the adjacent islands (Vaughan and Doake, 1996; Cook et al., 2005). In this eco-region, denominated Maritime Antarctica, processes occurring in glaciers and snow packs are closely interrelated with terrestrial and marine ecosystems. Thus, melting of massive snow/ice accumulations and its consequent run-off have impact on the physical and biological processes of the catchment areas and the near-shore marine environments that are not well known (Vogt and Braun, 2004).

Snow provides habitats for a variety of microorganisms, such as microalgae (Fujii et al., 2010; Harding et al., 2011), which can generate blooms thus coloring the snow red or green according to their life stage

\* Corresponding author at: Instituto de Ciencias Marinas y Limnológicas, Facultad de Ciencias, Universidad Austral de Chile, Valdivia, Chile.  
E-mail address: [pirjo.huovinen@uach.cl](mailto:pirjo.huovinen@uach.cl) (P. Huovinen).

<https://doi.org/10.1016/j.isprsjprs.2018.10.015>

Received 27 April 2018; Received in revised form 25 October 2018; Accepted 28 October 2018

0924-2716/ © 2018 International Society for Photogrammetry and Remote Sensing, Inc. (ISPRS). Published by Elsevier B.V. All rights reserved.

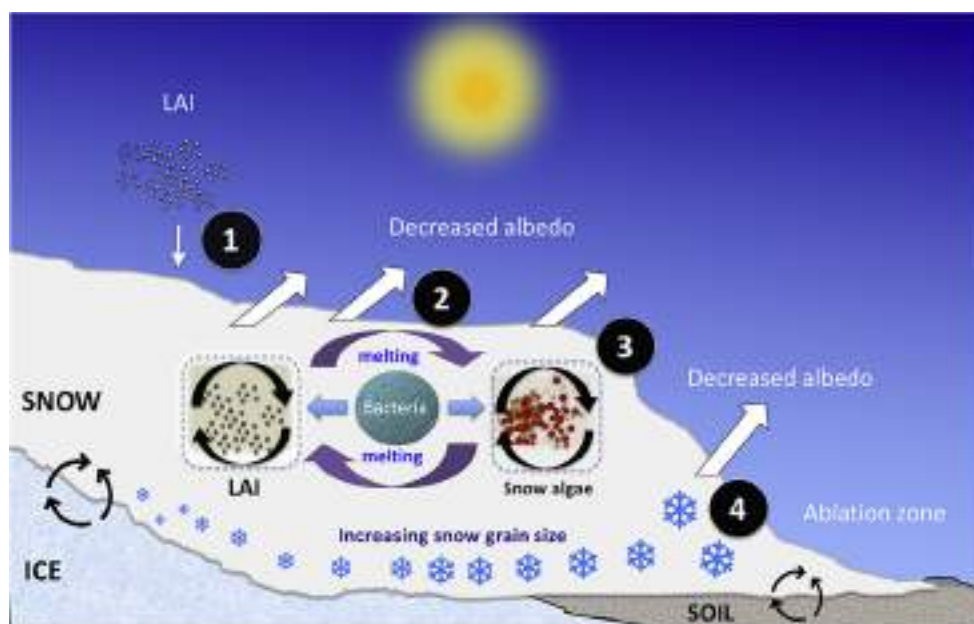


**Fig. 1.** Synthesis of the proposed feedback processes, which accelerate reduction of albedo in the ablation zone (see the text for references). (1) Atmospheric deposition of **light-absorbing impurities (LAI)** (such as black carbon, soot and dust) in the snow where they absorb light and cause warming, thus reduce albedo and induce melting of snow, which can result in concentration of LAI at the ice surface. (2) **Microorganisms** (e.g. bacteria and cyanobacteria), which can decrease albedo and are closely associated with snow algal communities, may bind to particulates (LAI) maintaining them at the surface layers. (3) **Snow algae**, favored in ablation zones as melting provides suitable environments for growth, absorb light thus reducing albedo and in turn exacerbating melting. Color that algae give to the snow is associated with the dominant pigments related with the life cycle stage (e.g. the cyst stage of some green algae with high concentration of carotenoids giving a red color, whereas in the vegetative stage green color dominates). (4) **Melting** of snowpack affects

albedo as drier, fresh snow with smaller grain size has higher albedo than wet snow with larger grain size. (For interpretation of the references to color in this figure legend, the reader is referred to the web version of this article.)

and pigment composition (Fig. 1). Changes in the physical-chemical characteristics of the snow pack are related to these different ecological stages where the composition of microalgae and associated bacteria can change considerably (Laybourn-Parry et al., 2013). In terms of optical properties of the snow, the microbial communities overall contribute to reducing albedo and increasing snow melting (Yallop et al., 2012; Lutz et al., 2014; Musilova et al., 2016; Ganey et al., 2017). Albedo values around 41–57% have been reported for red snow (Thomas and Duval, 1995; Lutz et al., 2014) and in the Arctic, it has been estimated to cause a 13% decrease in albedo during one melt season, increasing melting rates (Lutz et al., 2016). Thus, the importance of considering “bio-albedo” caused by snow microalgal communities in climate models has been emphasized recently (Lutz et al., 2016; Cook et al., 2017a, 2017b). Although the phenomenon of red snow has been known since centuries, better understanding is still needed on the life history, seasonality, ecology and distribution of these organisms and how they influence the biogeochemical processes in these ecosystems (Hoham and Duval, 2001; Hodson et al., 2017). Under the actual changing environmental scenarios (Turner et al., 2016; Oliva et al., 2017), snow microbial communities have to adapt to new regimes of melting and freezing (Dove et al., 2012), underlining not well-understood molecular and physiological adaptations.

Knowledge on the temporal and spatial scales of polar snow algal blooms is limited, e.g. due to remoteness and difficult access to the habitats, however, is needed in order to develop more accurate global change predictions that include bio-albedo. The use of satellite-derived data has opened improved opportunities for larger scale observations. Although remote sensing techniques have been widely used for estimation of terrestrial vegetation dynamics, recently also in the Antarctica (Fretwell et al., 2011; Shin et al., 2014; Vieira et al., 2014; Casanovas et al., 2015), to our knowledge only few studies on snow algae exist, mostly focused on red snow. Painter et al. (2001) were among the first ones to quantify snow algae using images from airborne spectrometer. Dozier and Painter (2004) addressed the impact of snow algae on surface reflectance on a glacier. Takeuchi et al. (2006) reported spatial distribution and abundance of red snow on an ice field in Alaska using the reflectance ratio of 610–680 (red) and 500–590 (green) nm bands of SPOT satellite. This proposed red/green ratio was recently applied to map red snow around the Russian Arctic and other sites (Hisakawa et al., 2015). On the other hand, satellite-derived data

have been used to describe the relative overall impurities in the snow, likely covering also microalgae (Dumont et al., 2014). Distinguishing different light-absorbing components, i.e. microbiota, inorganic and organic impurities, using satellite bands is challenging as e.g. dirt and carotenoid pigments have resembling effect on the reflectance spectrum of snow (Painter et al., 2001). In fact, reflectance ratios of red and green satellite bands have been used for measuring mineral dust (normalized band ratio; Di Mauro et al., 2015) and abundance of algae in the snow (Takeuchi et al., 2006; Ganey et al., 2017), indicating overlapping spectral reflectance signals, especially when using multispectral instead of hyperspectral instruments. While the potential of both snow microbiota and impurities to reduce albedo and accelerate snow melt are recognized (e.g. Cook et al., 2017b), recent reports have suggested their highly complex, and still largely unidentified and unquantified interactions and feedback processes within the snowpack (Lutz et al., 2014; Tedesco et al., 2016; Anesio et al., 2017; Tedstone et al., 2017) (Fig. 1). This emphasizes the need for more precise satellite-based identification techniques for different snow darkening compounds.

In the present study, the presence of microalgae and impurities in the snow of Fildes Peninsula, King George Island, West Antarctic Peninsula, was mapped through Sentinel-2A satellite images. Considering the heterogeneous characteristics of the snow in this area, data were analysed with Spectral Mixture Analysis (SMA) with the aim to map sub-pixel fractions of multiple components in mixed pixels (reviewed by Somers et al., 2011). Pixel abundance of snow algae and impurities from SMA were contrasted with satellite-derived snow albedo. In addition, the applicability of band ratios proposed for classifying snow algae (Red-Green band (R/G) ratio by Takeuchi et al. (2006) and impurities (Snow Darkening Index (SDI) by Di Mauro et al. (2015)) was tested and compared with SMA. Impurity Index ( $I_{imp}$ ) by Dumont et al. (2014) was additionally applied. Ground verification (characterization of microalgal composition in the snow samples using fluorometric analysis and spectral absorption of solar radiation by red and green snow samples) was made in two areas (Ardley Peninsula and Collins Glacier). The objectives were (1) to compare the effectiveness of SMA and different band ratios in mapping snow algae from satellite-derived data and distinguishing them from other snow-darkening impurities; and (2) to compare the relative impact of snow algae and other impurities (based on SMA) on albedo. Overall, this approach provides improved tools for modeling the reduction of albedo in different climate

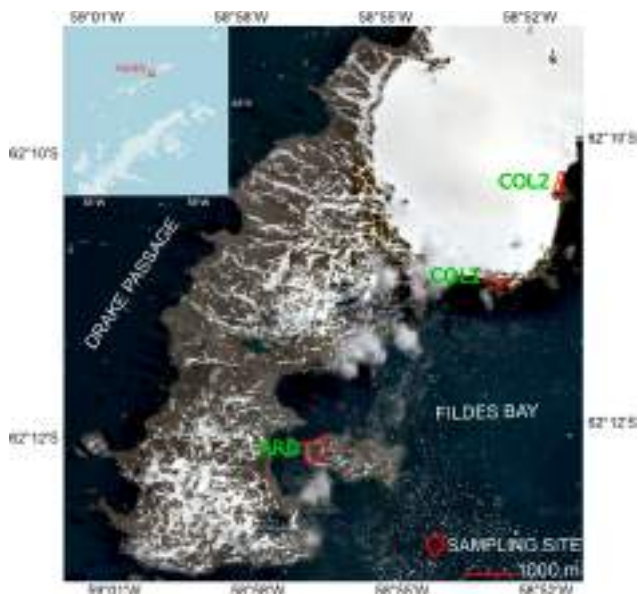


**Fig. 2.** Study site in Fildes Peninsula in the King George Island, Antarctica. Analyses of the satellite images were made for the area without the top of the Collins Glacier (saturation of pixels due to high reflectance on the glacier surface). Ground validation and testing was realized in three sites (ARD, COL1, COL2).

change scenarios and add unprecedented information how these microorganisms modify the optical features of Antarctic snow at different spatial and temporal scales.

## 2. Materials and methods

### 2.1. Study area and satellite-derived data processing

Satellite images covering the Fildes Peninsula, King George Island (62°12'S) (Fig. 2), coinciding the summer 2017 field campaign (see below) and presenting clear conditions for the major part of the area, were selected. Images of surface reflectance from Sentinel-2A Multi-Spectral Instrument (MSI) (19 January) were obtained from the free access page of NASA (<https://earthexplorer.usgs.gov/>). Map projection was WGS 84/UTM zone 21 s. Atmospheric correction was carried out through the module Sen2cor, included in the free disposal software Sentinel Application Platform (SNAP) provided by the European Space Agency (ESA) in the STEP platform (<http://step.esa.int/main/>). In order to mask clouds, cirrus, their shadows and water, the masks provided by Sen2cor level-2A algorithm Scene Classification (SCL masks) were used and confirmed with visual inspection. The characteristics of satellite bands are summarized in Table 1. Resampling was carried out with SNAP to transform spatial resolution from 20 m to 10 m.

The areas affected by clouds and their shadows in the eastern side of the peninsula (Fig. 2) were excluded from the analyses (approximately 5% of the surface area). The image analyses were made excluding major part of the Collins Glacier (also known as Bellingshausen Ice Dome) due to the saturation of pixels caused by the high reflectance on the glacier surface.

Snow coverage for the study area was calculated using green and short wavelength infrared (SWIR) bands according to the algorithm of Dozier (1989), defined as **Normalized Difference Snow Index (NDSI)** (Hall et al. (1995) (see Tables 1 and 2). The pixels with NDSI > 0.4 (to mask out of water) (Hall et al., 1995) and reflectance of NIR band > 0.11 were classified as snow or ice (Sibandze et al., 2014; Table 2).

In the area classified as snow, the presence of algal pigments, clean snow, debris and impurities was estimated using Spectral Mixture Analysis (SMA; see below) and band ratios (Table 2). **Spectral Mixture**

**Table 1**

Characteristics of the bands of Sentinel-2A used for spectral mixture analysis (SMA) and the calculation of the indices ( $\lambda$ ). The 20 m pixels bands were transformed to 10 pixels by resampling (SNAP).

Band number	Waveband (nm)	Central $\lambda$ (nm)	Resolution (m)	Characteristics
2	440–538	490	10	Blue <sup>a</sup>
3	537–582	560	10	Green <sup>a</sup>
4	646–684	665	10	Red <sup>a</sup>
5	694–713	705	20	Vegetation
6	731–749	740	20	Vegetation
7	769–797	783	20	Vegetation
8	760–908	842	10	NIR <sup>a</sup>
8a	848–881	865	20	Vegetation
11	1539–1682	1610	20	SWIR1 <sup>a</sup>
12	2078–2320	2190	20	SWIR2 <sup>a</sup>

<https://earth.esa.int/web/sentinel/user-guides/sentinel-2-msi/resolutions/spatial>.

**Analysis (SMA)** (Adams et al., 1986; Keshava and Mustard, 2002) was carried out using the Spectral unmixing tool of SNAP 6.0 software. The endmembers were selected from the whole Peninsula Fildes area based on known pigment spectra (see Fig. 3), and on published spectra for snow (Dozier, 1989; Wiscombe and Warren, 1980), impurities and debris (Warren and Wiscombe, 1980; Di Mauro et al., 2017; Kokhanovsky et al., 2018). For each category 34–107 endmembers representing pure pixels were selected. Then, mean of each category was used as an endmember in a linear mixture model (LMM) providing information on the endmember abundance (0–100%) (fractions of the endmembers).

**Albedo** was calculated for the snow covered area according to the algorithm of Liang (2001) created for Landsat-7, but applied also for Sentinel-2 images (Naegeli et al., 2017). **Red-Green band ratio (R/G)** as an indicator of red snow according to Takeuchi et al. (2006) was used, where ratio > 1.02 is considered an indicator of red snow. In addition, to distinguish the amount of algae, categories of 1.02–1.04 (low), 1.04–1.08 (medium), 1.08–1.12 (high) and > 1.12 (very high) were applied (Takeuchi et al., 2006). The presence of mineral dust in the snow was estimated with the **Snow Darkening Index (SDI)** described by Di Mauro et al. (2015) using normalized difference between surface reflectance in red and green bands (Table 2). In addition, the **Impurity Index ( $i_{imp}$ )**, introduced by Dumont et al. (2014), was calculated using green and NIR bands (Table 2).

### 2.2. Field verification

Snow samples with green and red coloration were collected during the austral summer (January 2017) in Peninsula Ardley and the frontal moraine of Collins Glacier in the Fildes Peninsula (Fig. 2). Samples of the upper layer (max. 10 cm thick) of snow with visible coloration were collected with a stainless-steel shovel. The samples were stored in plastic bags and transported in cooling box to the laboratory of the station “Base Profesor Julio Escudero” within few hours, where they were stored in the darkness at 2 °C and processed the following day.

Spectral absorbance of solar irradiation in snow samples was measured with a RAMSES-ACC2-UV-Vis Hyperspectral radiometer (TRIOS Optical Sensors, Oldenburg, Germany). Snow samples (cores of 7 cm diameter, 5 cm depth) were punched with a polypropylene tube from white, red and green snow. The snow blocks were placed on a UV-transparent Plexiglas plate, which was mounted on the sensor of the radiometer. The irradiance spectrum below the snow sample was contrasted with measurements in the air.

The relative composition of the principal algal groups, based on chlorophyll-*a* content *in vivo*, was evaluated in the laboratory from melted snow samples with the PHYTO-PAM-II chlorophyll fluorometer (Compact version, Heinz Walz GmbH, Germany), which differentiates

**Table 2**

Algorithms and satellite bands used to calculate Normalized Difference Snow Index (NDSI), Impurity Index ( $I_{imp}$ ), Snow Darkening Index (SDI), Red-Green band ratio (R/G) and albedo.

Index	Algorithm	Sentinel band	Criteria
NDSI	$(Green-SWIR)/(Green + SWIR)^{1,2}$	B3, B11	$NDSI > 0.4$ ; $NIR > 0.11$ snow <sup>7</sup>
$I_{imp}$	$\ln(Green)/\ln(NIR)^3$	B3, B8	
SDI	$(Red-Green)/(Red + Green)^4$	B4, B3	$SDI < 0$ (clean snow), $SDI > 0$ (dirty snow)
R/G	$Red/Green^5$	B4, B3	$R/G > 1.02$ red algae
Albedo	$0.356 * Blue + 0.130 * Red + 0.373 * NIR + 0.085 * SWIR1 + 0.072 * SWIR2 - 0.0018^6$	B2, B4, B8, B11, B12	Scale 0–1

<sup>1</sup> Dozier (1989).  
<sup>2</sup> Hall et al. (1995).  
<sup>3</sup> Dumont et al. (2014).  
<sup>4</sup> Di Mauro et al. (2015).  
<sup>5</sup> Takeuchi et al. (2006).  
<sup>6</sup> Liang (2001).  
<sup>7</sup> Sibandze et al. (2014).

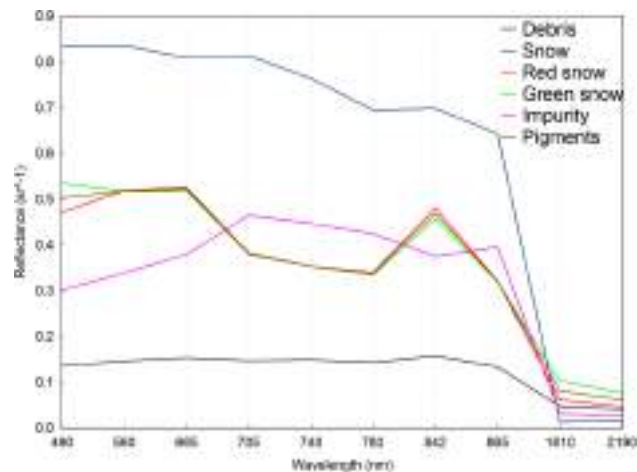


**Fig. 3.** Spectral reflectance (mean,  $n = 34$ – $107$ ) of algal pigments, impurities, debris and clean snow derived from pure pixels in Peninsula Fildes area and used as endmembers in SMA. In the testing sites (Ardley and Collins), endmembers for red and green snow pigments were used additionally. For end-member selection see text for details. (For interpretation of the references to color in this figure legend, the reader is referred to the web version of this article.)

cyanobacteria, green, brown (diatoms/dinoflagellates) and phycoerythrin containing (e.g. cryptophytes) algae. The measuring is based on the excitation of the sample with five measuring light wavelengths (440, 480, 540, 590 and 625 nm), which results in five fluorescence signals reflecting the absorbance spectra of antenna pigment arrangement of these four algal groups (Jakob et al., 2005). In addition, qualitative microscopic observation of the snow samples was carried out.

The research in the Antarctic was carried out under the permission granted by Instituto Antártico Chileno (INACH) in accordance with the Protocol on Environmental Protection to the Antarctic Treaty.

**2.3. Validation of classifications and accuracy assessment**

Accuracy of the classifications was tested in three testing sites (one site in Ardley covering 146 pixels, two sites in Collins covering 105 and 107 pixels) (Fig. 2). The pixels used as endmembers were not included in testing. Accuracy of the classification of each pixel in the testing areas was determined by contrasting the spectral reflectance of the pixel with that of the assigned endmember. The dominant type (> 50% abundance) confusion matrix was used to estimate user, producer and overall accuracy (Congalton and Green, 2009).

**3. Results**

**3.1. Field verification**

The presence of snow algae in the testing sites was confirmed by visual (field and microscopy) observations (Fig. 4A) and with chlorophyll *a* fluorescence based estimations of functional groups in the snow samples, revealing green microalgae as the dominant algal group (60–95%) in all the snow samples, followed by *Cyanobacteria*, which represented 40% of the algal composition in the red snow of Collins Glacier (Fig. 4C). In the snow samples of Ardley Peninsula (15–22%) and in green snow of Collins Glacier (5%) *Cyanobacteria* were less dominant. In the green snow of Ardley Peninsula, other algal groups (diatoms and phycoerythrin containing algae) were also detected (5% each) (Fig. 4C). Higher maximal chlorophyll *a* concentrations (total of all algal groups) were found in green snow samples (mean up to  $2 \text{ mg l}^{-1}$ ) than in red snow (up to  $0.8 \text{ mg l}^{-1}$ ).

Classification derived from SMA in the pixels in the ground validation areas indicated dominance of red snow (red cyst algal stages) in Glacier Collins (deeper and larger snow packs) and relatively higher proportion of green snow (vegetative algal stages) in Peninsula Ardley (characterized by smaller snow patches) (Fig. 4B). This is in agreement with the observed patterns in the field: in Ardley Peninsula small patches of snow dominated providing more wet habitats for vegetative algal stages, while Glacier Collins site was characterized by more extensive and deeper snow packs implying drier habitats with dominance of red cyst stages (Fig. 4A). Green snow from Ardley Peninsula contained a wide variety of microalgae, reflecting the nutrient-rich environment and the presence of also other than true snow algae, introduced temporarily from the surrounding environment (Fig. 4A and C). Spectral reflectance from SMA (Fig. 4B) confirmed a higher absorption in the carotenoid and phycocyanin range (see Fig. 5) in red snow than in green snow, coinciding with the presence of red cyst algal stages and cyanobacteria (Fig. 4A and C).

Based on SMA, 72% of the pixels in Ardley and 45% in Collins presented pigment features (over 10% abundance), whereas corresponding impurity coverage were 44% and 36%, respectively (Table 3). The presence of dark inorganic particles at the snow surface could be visually confirmed (Fig. 4A).

The presence of algae in the snow was shown to modify the spectral absorption of solar radiation (Fig. 5). The top 5-cm layer of white snow absorbed around 30% of PAR (400–700 nm), while absorption increased towards UV-B radiation (up to 60%). Red and green snow showed overall high absorptance of solar irradiation in comparison with white snow, absorbing almost completely radiation at UV and blue wavelengths (< 500 nm). The differences between the red and green snow were mainly observed in the 500–650 nm range with higher absorptance of red snow, reflecting the absorption by carotenoids around

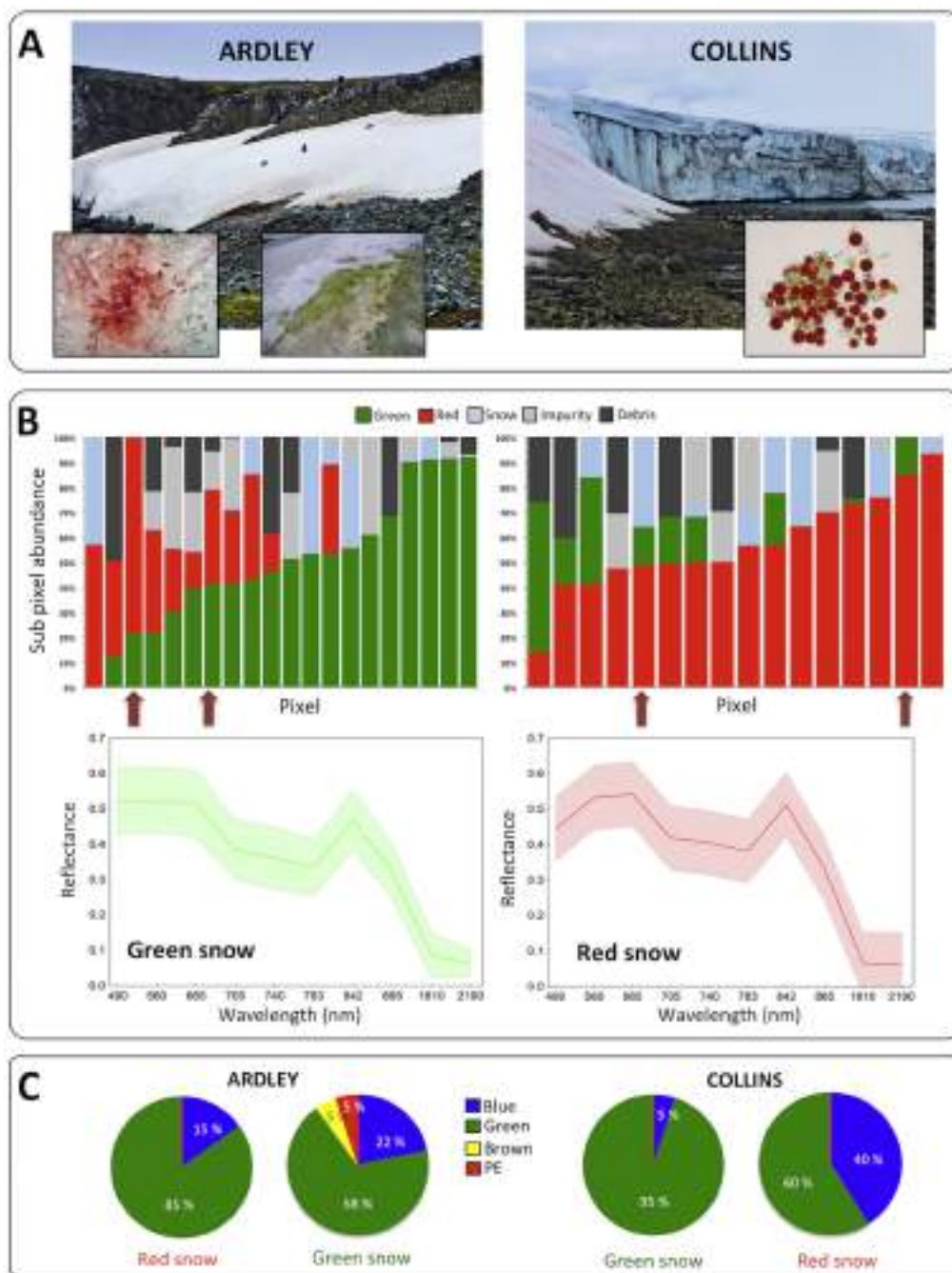


**Fig. 4.** Overview of the ground verification and sampling sites in Peninsula Ardley and Glacier Collins area (A). Composition of light absorbing snow components based on SMA in Ardley and Collins (COL2) testing sites in pixels classified with dominance of pigments (> 50%). Arrows indicate the areas of snow algal samplings. Spectral reflectance (mean ± SE) of the pixels with green (n = 29) and red (n = 11) snow dominance used as endmembers in SMA (B). Composition of principal phytoplankton groups (cyanobacteria, green, brown (diatoms/dinoflagellates) and phycoerythrin (PE) containing algae) (mean, n = 6–12) based on chlorophyll-a content with the PHYTO-PAM fluorometer in the red and green snow from Collins Glacier and Ardley Peninsula (C). Photography: D. Osman; Microscopy: P. Huovinen. (For interpretation of the references to color in this figure legend, the reader is referred to the web version of this article.)

500–510 nm, as well as by phycoerythrin and phycocyanin present in cyanobacteria associated with red snow (Fig. 4C, 5). Both green and red snow showed higher absorbance around 675 nm (coinciding with chlorophyll), while at 700 nm red snow had higher absorbance (90%) compared to green snow (80%) (Fig. 5).

### 3.2. Accuracy assessment of the classifications

Based on user accuracy (92%), SMA resulted a reliable method to classify snow algae with low (8%) false positive classifications. On the other hand, producer accuracy (63%) derived from dominant type (> 50% abundance) confusion matrix indicated an omission error, i.e. 37% underestimation of snow algae (Table 4).

Comparison between testing sites showed lower producer accuracy in Collins (35–54%) than in Ardley (83%) (Table 5). Classification of

impurity also presented higher user (93%) than producer (53%) accuracy (Table 4). In contrast, classification of clean snow and debris had low user accuracy (26–27%; frequent false positives) and high producer accuracy (76–91%; low omission error) (Table 4). Especially in Ardley characterized by patchiness of snow, the classification of pure snow was not reliable (user accuracy only 6%) (Table 5). Overall accuracy (61%) was affected by the low user accuracy of snow and debris as well as the unclassified pixels (Table 4).

Snow algal classification with R/G ratio resulted in larger number of false positives than correct classifications (user accuracy 46%) (Table 6). Omission error was even higher (producer accuracy 36%). Impurity classification with SDI showed a better producer accuracy (68%) with lower omission error, however, also was affected by false positive classifications (user accuracy 36%). Overall accuracies were 46% (R/G) and 57% (SDI) (Table 6).

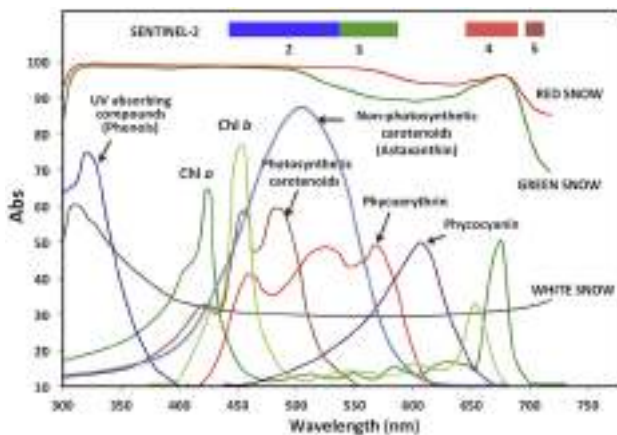


**Fig. 5.** Spectral absorbance of solar irradiation in a 5-cm layer of white, red and green snow (relative to the measurement in the air) using a UV-Vis hyperspectral radiometer. General absorption spectra of the main photosynthetic pigments and UV-absorbing compounds in algae are given (see e.g. Bricaud et al., 2004). Sentinel-2A bands coinciding this spectral range are indicated. (For interpretation of the references to color in this figure legend, the reader is referred to the web version of this article.)

**Table 3**

Snow coverage (%) in Fildes Peninsula (without Collins Glacier) and in the testing sites (Ardley Peninsula (ARD; 146 pixels) and Collins Glacier (COL; 212 pixels); Fig. 2) evaluated from image of Sentinel-2A. Coverage (%) of impurities and algae in the snow, based on Impurity ( $I_{imp}$ ), Snow Darkening (SDI), Normalized Difference Snow (NDSI) and Red-Green band ratio (R/G) as well as on pigment and impurity from spectral mixture analysis (SMA).

	Fildes	ARD	COL
<i>Snow coverage</i>	35.2		
<i>SMA pigments</i>			
> 50%	18.6	55.5	20.8
10–40%	23.9	16.4	24.5
<i>SMA impurity</i>			
> 50%	14.7	17.1	16.0
10–40%	14.5	26.7	20.3
<i>R/G</i>			
1.02–1.4	25.7	35.6	44.3
1.02–1.04 (low)	6.4	7.5	8.5
1.04–1.08 (medium)	8.3	15.8	12.3
1.08–1.12 (high)	4.8	4.8	8.5
1.12–1.4 (very high)	6.2	7.5	15.1
<i>SDI</i>			
–0.14 to 0 (clean snow)	65.3	47.9	45.3
0–0.18 (dirty snow)	34.7	52.1	54.7
0–0.05	27.1	43.8	37.3
0.05–0.1	6.3	8.2	11.3
0.1–0.18	1.3	0.0	6.1
<i>IMP</i>			
0–0.5	17.3	0.7	9.0
0.5–1	61.9	71.2	56.6
1–1.2	13.0	28.1	23.1

### 3.3. Mapping algae and impurities in snow

In January 2017, 35% of the Fildes Peninsula (area without Collins Glacier) was covered with snow (Table 3). Based on SMA, approximately 19% of the snow was dominated by algae (over 50% pixel abundance), reaching 43% when considering > 10% pixel abundance (Table 3, Fig. 6). Based on R/G ratio, 26% of the snow was classified as containing algae, divided rather evenly into four amount categories (5–8% each) (Table 3, Fig. 7). Based on SMA, around 15% of the snow was dominated by impurities (over 50% pixel abundance) (Table 3, Fig. 6).

According to SDI, 35% of this snow contained mineral dust (SDI > 0), while 65% could be classified as clean snow (SDI < 0) (Table 3, Fig. 7).

Combining snow algae and impurities based on SMA (Fig. 8A) and indices (R/G,  $I_{imp}$ ; Fig. 8B) together with clean snow (from SMA) in RGB images allows visualizing their distribution in the study area. SMA provided higher precision in separating algae, impurities and clean snow (Fig. 8A) than R/G and impurity index ( $I_{imp}$ ) (Fig. 8B), which resulted in higher degree of overlapping signals in mixed pixels, with low level of precision in identification of the dominant LAI.

Highest albedo (> 65%) values could be associated with areas of clean snow (Fig. 9A). When snow algae were the dominant light-absorbing component (100% pixel abundance), observed albedo decreased to approximately 45% (Fig. 9F), while the dominance by impurities decreased albedo down to 30% (Fig. 9C). These albedo values turned out to be thresholds for tendencies between decrease in albedo vs. increase in abundance of algae or impurity observed towards higher albedo levels (> 45% for pigments (Fig. 9F) and > 30% for impurity (Fig. 9C)), which were mainly concentrated to the central areas of the snow packs. At lower albedo levels, coinciding snow line areas, weaker or opposite trends were observed (Fig. 9B and D).

## 4. Discussion

### 4.1. Effectiveness of SMA vs. band ratios in mapping algae and other snow-darkening impurities from satellite imagery

One of the major challenges in remote sensing of snow-darkening is distinguishing the contribution of snow algae from other light-absorbing compounds as one pixel area can cover a wide range of overlapping signals from a variety of sources. With this respect, the area of Fildes Peninsula is challenging as it presents variations in the topography and geomorphology (Schmid et al., 2016). The seasonal patchiness of the snow cover, especially in ice-free coastal areas, increases along with the melting and results in patches that are smaller than the spatial resolution of many satellite images. On the other hand, high reflectance on areas such as the surface of Collins Glacier causes saturation of pixels, a phenomenon that typically occurs over glaciers and snowfields (Takeuchi et al., 2006). Furthermore, the climatic conditions often limit the availability of clear satellite images in this geographical region.

Spectral unmixing proved to be a promising tool to discriminate different light-absorbing components in the snow. This type of methods have been widely used e.g. in land cover classifications as they allow sub-pixel level classification in mixed pixels (reviewed by Somers et al., 2011). Thus, proportional abundance of different components within a pixel is obtained, whereas the use of band ratios or algorithm-based indices results in one classification category per pixel. Therefore for heterogeneous habitats, such as snow, spectral unmixing offers a clear advantage, and in fact, in the present study this method provided good user accuracy in pigment and impurity classification. On the other hand, omission error was higher. This can be attributed at least partly to the use of dominant type (> 50% abundance) confusion matrix for accuracy assessment, which considers pixels with lower pigment coverage (< 50% abundance) false classifications. This can lead to site-specific differences: the lower coverage of pigment-dominated pixels in Collins testing site apparently resulted in lower producer accuracy in this site as compared to the Ardley testing site with higher pigment coverage. In order to minimize this type of misinterpretations of the accuracy, sub-pixel fractional error matrices have been proposed for mixed pixels (Latifovic and Olthof, 2004). Classification of clean snow resulted in more misclassifications than pigments and impurities as the variety of endmembers did not represent widely enough the different snow types present in Peninsula Fildes. Here, multiple endmembers representing different snow types could improve this aspect (e.g. using MESMA; proposed by Roberts et al., 1998).

**Table 4**

Accuracy assessment of spectral mixture analysis (SMA) derived from the dominant type (> 50% abundance) confusion matrix. Classified data are given in the rows and reference data in the columns, diagonal (gray shade) indicating the correctly classified pixels for each category. Data (as number of pixels) from all testing sites are combined (see Table 5 for individual sites).

Classified data	Reference data				Unclassified	Total	User accuracy (%)
	Algae	Impurity	Debris	Snow			
Algae	115		5		5	125	92
Impurity	1	55			3	59	93
Debris	28	11	16	1	6	62	26
Snow	27	28		21	2	78	27
Unclassified	11	9		1	13	34	38
Total	182	103	21	23	29	358	
Producer accuracy (%)	63	53	76	91	45		
Overall accuracy (%)							61

**Table 5**

Accuracy assessment of spectral mixture analysis (SMA) for the three testing sites derived from the dominant type (> 50% abundance) confusion matrix (see Table 4 for details).

	Producer accuracy (%)	User accuracy (%)	Overall accuracy (%)
<b>ARDLEY</b>			70
Algae	83	88	
Impurity	58	88	
Debris	29	22	
Snow	100	6	
Unclassified	43	43	
<b>COLLINS 1</b>			57
Algae	54	100	
Impurity	43	91	
Debris	100	30	
Snow	100	40	
Unclassified	40	33	
<b>COLLINS 2</b>			54
Algae	35	100	
Impurity	55	100	
Debris	–	–	
Snow	90	32	
Unclassified	60	38	

**Table 6**

Accuracy assessment of the classification with indices (R/G, SDI) derived from the confusion matrix. Classified data are given in the rows and reference data in the columns, diagonal (gray shade) indicating the correctly classified pixels for each category (presence (Yes) or absence (No) of algae (R/G) or mineral dust (SDI)). Data (as number of pixels) from all testing sites are combined.

Classified data	Reference data			User accuracy (%)
	Yes	No	Total	
<b>R/G</b>				
Yes	66	79	145	46
No	116	97	213	46
Total	182	176	358	
Producer accuracy (%)	36	55		
Overall accuracy (%)				46
<b>SDI</b>				
Yes	70	122	192	36
No	33	133	166	80
Total	103	255	358	
Producer accuracy (%)	68	52		
Overall accuracy (%)				57

In the present study, red/green (R/G) band ratio proposed by Takeuchi et al. (2006) for red snow and normalized difference index SDI proposed by Di Mauro et al. (2015) for snow darkening gave low accuracy for pigment and impurity classification. R/G band ratio suffered both from incorrect classifications and omission errors, while SDI suffered mainly from incorrect classifications. Although Takeuchi et al. (2006) and Di Mauro et al. (2015) were able to validate the use of these band ratios against ground measurements of red snow (Takeuchi et al., 2006) and mineral dust (Di Mauro et al. (2015), overlapping reflectance signals can be expected as the same satellite bands (red and green) are used. In fact, the normalized difference index proposed by Di Mauro

et al. (2015) for mineral dust has also been related to snow algae (Ganey et al., 2017). Indeed, the impact of dirt on the reflectance spectrum of snow has been shown to resemble that of carotenoid pigments and can therefore interfere with the reliable detection of snow algae (Painter et al., 2001). Thus, it could be argued that the use of red and green bands (normalized difference index or band ratio) does not allow a detailed identification of the snow darkening components, and recent reports on the coverage of red snow in the Arctic snow and ice fields based on R/G ratio (Hisakawa et al., 2015) could be influenced by other snow darkening components.

#### 4.2. Impact of algae and other light-absorbing impurities in reducing snow albedo

The frontal moraine system and snow line of the Collins Glacier, raised beaches in the west Drake Passage coast (see Schmid et al. (2016) for geomorphology of Fildes Peninsula) and in general the ablation zones of snow packs could be identified as areas where highest coverage of pigments and snow darkening impurities in the snow coincided, together with low albedo. This is in agreement with the increasing grain size in melting snow with reduced albedo (Wiscombe and Warren, 1980), which is linked to the melt-induced growth of snow algae and their community dynamics (Lutz et al., 2014) (see Fig. 1). However, these zones turned out to be challenging environments when looking for patterns between albedo and snow darkening compounds as they in general already have low albedo (e.g. due to increasing grain size in melting/ageing snow) and any influence from snow-darkening compounds seemed to be masked by variations e.g. in snow characteristics or other environmental conditions. On the other hand, decreased albedo could be related with increased abundance of snow algae and other impurities at higher albedo levels, present mainly in the central areas of the snow packs. Overall, impurities could be estimated to have somewhat higher impact on reducing albedo (down to 30%) than snow algae (45%) in Fildes Peninsula. These albedo values for snow algae are in the range of previously reported for red (41–58%) and green (40–48%) snow (Thomas and Duval, 1995; Lutz et al., 2014). While the detection of snow algae is influenced by their seasonal, spatial, composition and life cycle variations (red, orange, green snow), also differences in the light-absorbing characteristics of impurities of different type and origin are likely to occur. In Fildes Peninsula, carbon soot from local sources (Na et al., 2011) is the most likely atmospheric impurity present in the snow, while in mid-latitudes snow may contain also desert dust (containing iron oxide) and soot from industrial origin, forest fires etc. (Warren and Wiscombe, 1980).

Although in Fildes Peninsula the physical and biological processes connecting different ecosystems are highly dynamic (Fan et al., 2013; Shevnina and Kourzeneva, 2017), our results confirmed the contrasting characteristics of the two ground validation sites. Snow patches in Ardley Peninsula are adjacent to a penguin colony and thus characterized by high biogenic nutrient loading and hence hosting a high biodiversity of snow inhabitants with dominance of green algae. Unlike

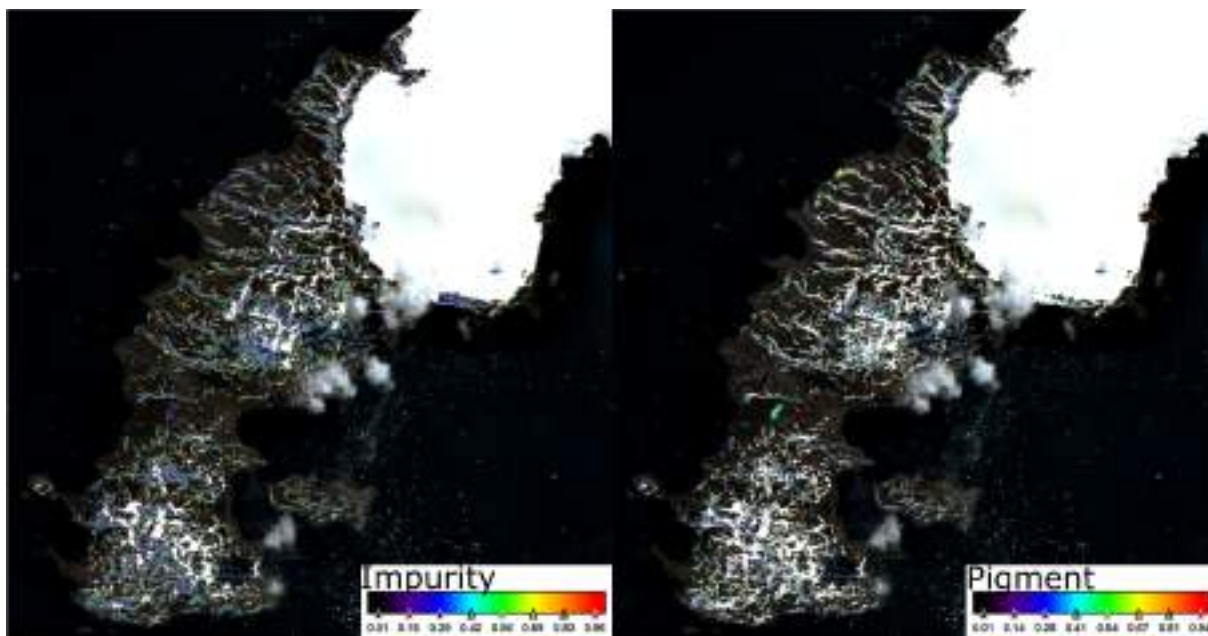


Fig. 6. Impurity and snow algal abundance (in scale 0–1) in Fildes Peninsula in January 2017 derived from Sentinel-2A images and analysed with SMA. Analyses were made without the top of the Collins Glacier (saturation of pixels due to high reflectance on the glacier surface; imaged here as white snow for clarity).

alpine and other continental snowfields, coastal snow packs in the Maritime Antarctica are normally eutrophic environments, mostly due to the presence of seabird and mammal colonies (Bidigare et al., 1993). Here, melt-water percolation through the snowpack causes a redistribution of organic matter regulated by a suite of physical-chemical and biological processes (e.g. bacterial degradation of debris) (reviewed by Tranter and Jones, 2001). Also, the influence of oceanic waters on the snow characteristics and communities can be expected in the wind and wave-exposed coastal sites. In contrast, the sites around Collins Glacier, due to different optical properties of the snow, apparently are more strongly influenced by physical factors such as high solar radiation and low nutrient concentrations, which promotes the prevalence of red snow (cyst algal stages) and cyanobacteria.

#### 4.3. Future projections

The improvements in the detection of bio-optical properties of snow microorganisms living in snow and ice fields will allow expanding our understanding on their role in the global climate change in Antarctica.

Snowfields are highly sensitive ecosystems and responsive to changes in environmental conditions (e.g. temperature, light and precipitations), and thus they can be regarded as excellent model ecosystems to examine the impact of climate change. Warming in several regions has been related with lower precipitation as snow, earlier runoff and hence, a shortened period of snow permanence (Barnett et al., 2008). This phenomenon has important consequences for the regional climate due to changes in the radiative energy balance, temperature and albedo (Groisman et al., 1994; Brown and Mote, 2008) and is fundamental in order to understand the interannual variability of temperature and hydrological regimes at a global scale (Groisman and Davies, 2001; Déry and Brown, 2007). In order to be able to enter snow algae and LAI in the climate models, more precise tools for their remote detection are needed. Recent hypotheses related to the massive melting of the Greenland Ice Sheet point to the importance of feedback processes between snow and ice algae and LAI rather than their individual contribution (Tedesco et al., 2016). Thus there is increasing need to understand the role and interactions of different components of snowpack affecting albedo (see Fig. 1). As snow algae are more dependent on the

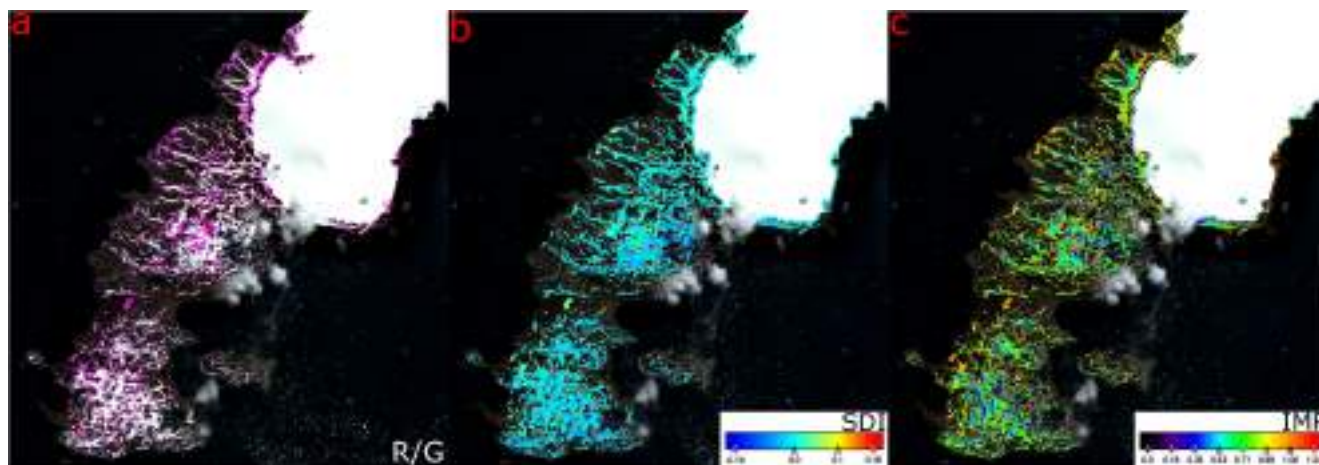


Fig. 7. Red-green (R/G), snow darkening (SDI) and Impurity ( $I_{imp}$ ) indices in Ardley Peninsula in January 2017 derived from Sentinel-2A images. Analyses were made without the top of the Collins Glacier (saturation of pixels due to high reflectance on the glacier surface; imaged here as white snow for clarity).

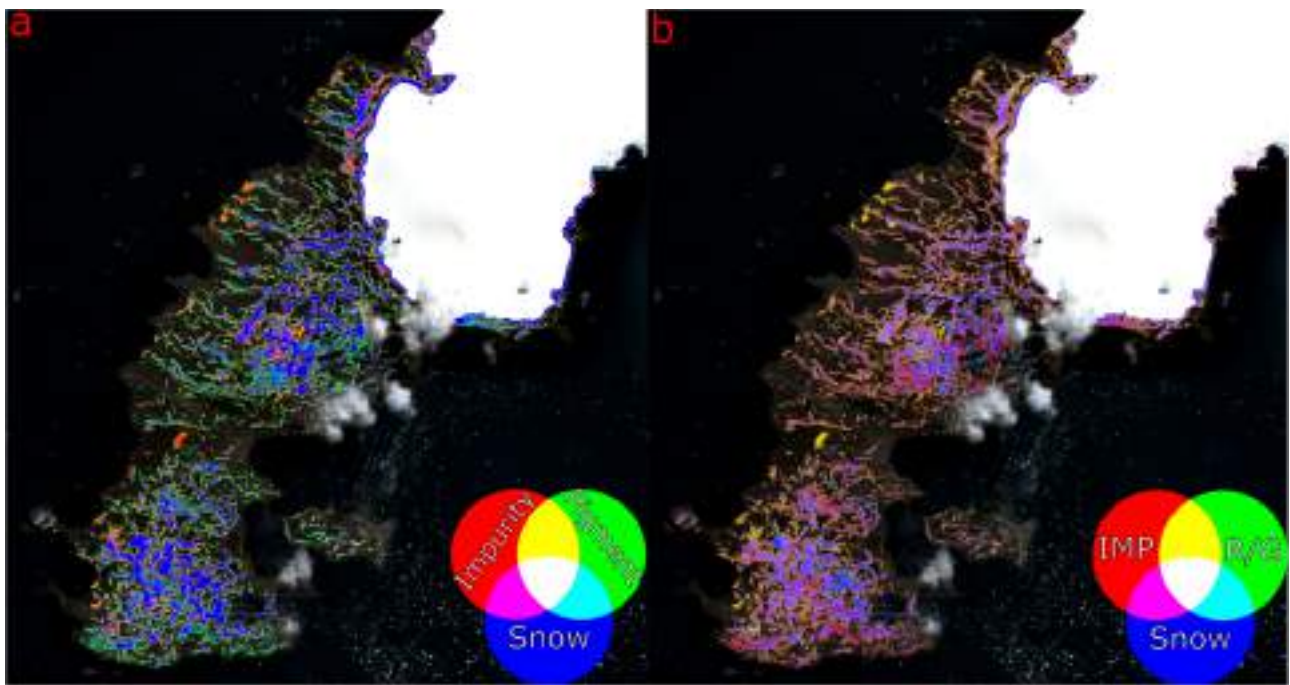


Fig. 8. RGB images integrating impurity, pigments and clean snow based on SMA (a), and impurity index ( $I_{imp}$ ), red-green (R/G) index and clean snow (based on SMA) (b) in Fildes Peninsula in January 2017 derived from Sentinel-2A images. Analyses were made without the top of the Collins Glacier (saturation of pixels due to high reflectance on the glacier surface; imaged here as white snow for clarity).

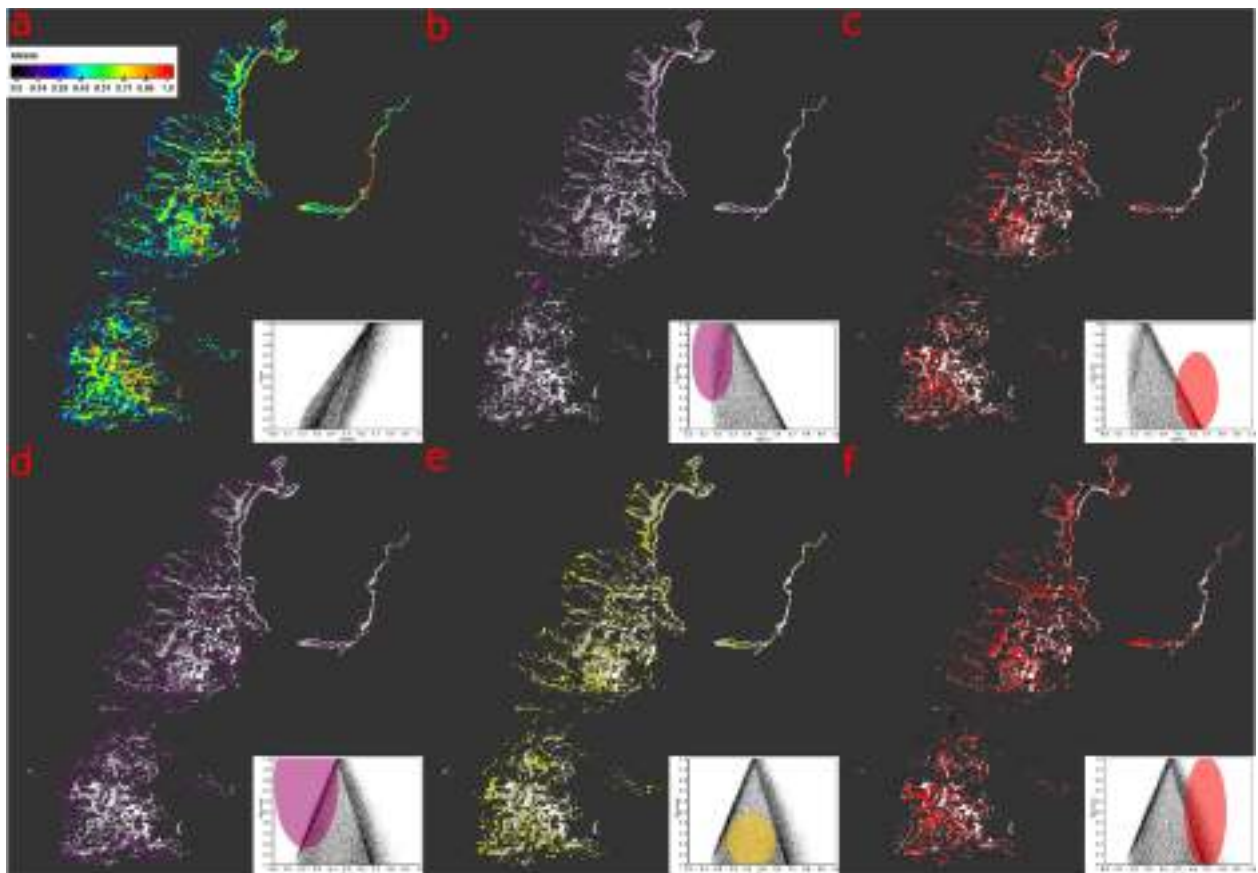


Fig. 9. Snow albedo (scale 0–1) in Fildes Peninsula in January 2017 derived from Sentinel-2A image (a). Scatter plot (using SNAP) of albedo against SMA-based clean snow (a), impurity (b and c) and pigment abundance (d–f) of all the pixels in the snow covered study area. For impurity (b and c) and pigments (d–f), different tendencies in the scatter plot associated with different types of geographical locations and environments (see the maps) are indicated in colors. (For interpretation of the references to color in this figure legend, the reader is referred to the web version of this article.)

conditions of their habitat (e.g. liquid water, light, nutrients) and present stronger seasonal variation in their dynamics than LAI, the feedback processes within the snowpack will be complex and temporally changing.

In all, analysis of remotely sensed data opens far-reaching opportunities to examine a series of parameters of snow microorganisms, which would not be possible through ground-based studies. In fact, the use of this technology in conjunction with observational, physiological and molecular approaches can become relevant to understand and estimate, not only their impact on albedo, but their biogeographical distribution, seasonality, biomass and primary production, and other biological processes in areas hitherto inaccessible to researchers.

#### 4.4. Conclusions

- Spectral Mixture Analysis (SMA) resulted a reliable method to classify snow algae and impurities with low level of false classifications. Omission error was somewhat higher, likely influenced by the dominant type confusion matrix in accuracy assessment.
- SMA provided higher precision in separating dominant light-absorbing impurities (LAIs) than the band ratios, which present widely overlapping signals.
- Classification of snow algae with Red/Green band ratio resulted in large number of both false positives and omission error, while classification of impurities with Snow Darkening Index (SDI) suffered mostly from false classifications.
- Highest albedo (> 65%) values were related with clean snow. Dominance of snow algae decreased albedo to 45%, while impurities decreased albedo to 30%, pointing to a major impact of latter in reducing albedo in Fildes Peninsula. Above these albedo thresholds, decrease in albedo could be linked with increase of algae or impurity.

#### Acknowledgements

This work was supported by CONICYT [FONDECYT grant N° 1161129 and FONDAPE grant N° 15150003]. The authors are grateful to D. Osman and C. Rivas for their invaluable help in the field work. The logistical support provided by the Instituto Antártico Chileno (INACH) and the staff at the Base Julio Escudero Station, as well as the contribution of the anonymous reviewers in improving the quality of this manuscript, is also greatly acknowledged. Copernicus Sentinel data [2017] for Sentinel data.

#### References

- Adams, J.B., Smith, M.O., Johnson, P.E., 1986. Spectral mixture modeling: a new analysis of rock and soil types at the Viking Lander 1 Site. *J. Geophys. Res.* 91, 8098. <https://doi.org/10.1029/JB091iB08p08098>.
- Anesio, A., Lutz, S., Christmas, N.A.M., Benning, L.G., 2017. The microbiome of glaciers and ice sheets. *npj Biofilms Microbiomes* 3, 10. <https://doi.org/10.1038/s41522-017-0019-0>.
- Barnett, T., Pierce, D., Hidalgo, H., 2008. Human-induced changes in the hydrology of the western United States. *Science* 319, 1080–1083.
- Benning, L.G., Anesio, A.M., Lutz, S., Tranter, M., 2014. Biological impact on Greenland's albedo. *Nat. Geosci.* 7, 691.
- Bigdare, R.R., Ondrusek, M.E., Kennicutt II, M.C., Iturriaga, R., Harvey, H.R., et al., 1993. Evidence for a photoprotective function for secondary carotenoids of snow algae. *J. Phycol.* 29, 427–434.
- Bricaud, A., Claustre, H., Ras, J., Oubelkheir, K., 2004. Natural variability of phytoplanktonic absorption in oceanic waters: influence of the size structure of algal populations. *J. Geophys. Res.* 109, C11010. <https://doi.org/10.1029/2004JC002419>.
- Brown, R., Mote, P., 2008. The response of northern hemisphere snow cover to a changing climate. *J. Clim.* 22, 2124–2145. <https://doi.org/10.1175/2008JCLI2665.1>.
- Casanovas, P., Black, M., Fretwell, P., Convey, P., 2015. Mapping lichen distribution on the Antarctic Peninsula using remote sensing, lichen spectra and photographic documentation by citizen scientists. *Polar Res.* 34, 25633. <https://doi.org/10.3402/polar.v34.25633>.
- Clarke, A., Johnston, N.M., Murphy, E.J., Rogers, A.D., 2012. Antarctic ecology in a changing world. In: Rogers, A., Johnston, N., Clarke, A., Murphy, E. (Eds.), *Antarctic Ecosystems: An Extreme Environment in a Changing World*. Wiley-Blackwell, Chichester, pp. 1–7.
- Congalton, R.G., Green, K., 2009. *Assessing the Accuracy of Remotely Sensed Data. Principles and Practices*. CRC Press, Boca Raton, pp. 183.
- Cook, A.J., Fox, A.J., Vaughan, D.G., Ferrigno, J.G., 2005. Retreating glacier fronts on the Antarctic Peninsula over the past half-century. *Science* 308, 541–544.
- Cook, J., Edwards, A., Takeuchi, N., Irvine-Fynn, T., 2016. Cryoconite: The dark biological secret of the cryosphere. *Prog. Phys. Geogr.* 40, 66–111.
- Cook, J.M., Hodson, A.J., Taggart, A.J., Mernild, S.H., Tranter, M., 2017a. A predictive model for the spectral “bioalbedo” of snow. *J. Geophys. Res. Earth Surf.* 122, 434–454. <https://doi.org/10.1002/2016JF003932>.
- Cook, J.M., Hodson, A.J., Gardner, A.S., Flanner, M., Tedstone, A.J., et al., 2017b. Quantifying bioalbedo: a new physically based model and discussion of empirical methods for characterizing biological influence on ice and snow albedo. *Cryosphere* 11, 2611–2632. <https://doi.org/10.5194/10.5194/10.11-2611-2017>.
- Déry, S.J., Brown, R.D., 2007. Recent northern hemisphere snow cover extent trends and implications for the snow-albedo feedback. *Geophys. Res. Lett.* 34, L22504. <https://doi.org/10.1029/2007GL031474>.
- Di Mauro, B., Fava, F., Ferrero, L., Garzonio, R., Baccolo, G., Delmonte, B., Colombo, R., 2015. Mineral dust impact on snow radiative properties in the European Alps combining ground, UAV, and satellite observations. *J. Geophys. Res. Atmos.* 120, 6080–6097. <https://doi.org/10.1002/2015JD023287>.
- Di Mauro, B., Baccolo, G., Garzonio, R., Giardino, C., Massabò, D., Piazzalunga, A., Rossini, M., Colombo, R., 2017. Impact of impurities and cryoconite on the optical properties of the Morteratsch Glacier (Swiss Alps). *Cryosphere* 11, 2393–2409. <https://doi.org/10.5194/10.5194/10.11-2393-2017>.
- Dozier, J., 1989. Spectral signature of alpine snow cover from the Landsat Thematic mapper. *Remote Sens. Environ.* 28, 9–22.
- Dozier, J., Painter, T.H., 2004. Multispectral and hyperspectral remote sensing of alpine snow properties. *Annu. Rev. Earth Planet. Sci.* 32, 465–494. <https://doi.org/10.1146/annurev.earth.32.101802.120404>.
- Dove, A., Heldmann, J., McKay, C., Toon, O.B., 2012. Physics of a thick seasonal snowpack with possible implications for snow algae. *Arct. Antarct. Alp. Res.* 44, 36–49.
- Dumont, M., Brun, E., Picard, G., Michou, M., Libois, Q., Petit, J.-R., Geyer, M., Morin, S., Josse, B., 2014. Contribution of light-absorbing impurities in snow to Greenland's darkening since 2009. *Nature Geosci.* 7, 509–512.
- Fan, J., Li, L., Han, J., Ming, H., Li, J., Na, G., Chen, J., 2013. Diversity and structure of bacterial communities in Fildes Peninsula, King George Island. *Polar Biol.* 36, 1385–1399.
- Fretwell, P.T., Convey, P., Fleming, A.H., Peat, H.J., Hughes, K.A., 2011. Detecting and mapping vegetation distribution on the Antarctic Peninsula from remote sensing data. *Polar Biol.* 34, 273–281. <https://doi.org/10.1007/s00300-010-0880-2>.
- Fujii, M., Takano, Y., Kojima, H., Hoshino, T., Tanaka, R., Fukui, M., 2010. Microbial community structure, pigment composition, and nitrogen source of red snow in Antarctica. *Microb. Ecol.* 59, 466–475.
- Ganey, G.Q., Loso, M.G., Bryant Burgess, A., Dial, R.J., 2017. The role of microbes in snowmelt and radiative forcing on an Alaskan icefield. *Nat. Geosci.* 10, 754–761. <https://doi.org/10.1038/NGEO3027>.
- Groisman, P.Y., Karl, T.R., Knight, R.W., Stenchikov, G.L., 1994. Changes of snow cover, temperature, and radiative heat balance over the Northern Hemisphere. *J. Clim.* 7, 1633–1656.
- Groisman, P., Davies, T.D., 2001. Snow cover and the climate system. In: Jones, H.G., Pomeroy, J.W., Walker, D.A., Hoham, R.W. (Eds.), *Snow ecology system*. In: Jones, H.G., Pomeroy, J.W., Walker, D.A., Hoham, R.W. (Eds.), *Snow Ecology. An Interdisciplinary Examination of Snow-covered Ecosystems*. Cambridge University Press, pp. 1–44.
- Hall, D.K., Riggs, G.A., Salomonson, V.V., 1995. Development of methods for mapping global snow cover using moderate resolution imaging spectroradiometer data. *Rem. Sens. Environ.* 54, 127–140. [https://doi.org/10.1016/0034-4257\(95\)00137-P](https://doi.org/10.1016/0034-4257(95)00137-P).
- Harding, T., Jungblut, A.D., Lovejoy, C., Vincent, W.F., 2011. Microbes in high Arctic snow and implications for the cold biosphere. *Appl. Environ. Microbiol.* 77, 3234–3243.
- Hisakawa, N., Quistad, S.D., Hester, E.R., Martynova, D., Maughan, H., Sala, E., Gavrilo, M.V., Rohwer, F., 2015. Metagenomic and satellite analyses of red snow in the Russian Arctic. *PeerJ* 3, e1491. <https://doi.org/10.7717/peerj.1491>.
- Hodson, A.J., Nowak, A., Cook, J., Sabacka, M., Wharfe, E.S., Pearce, D.A., Convey, P., Vieira, G., 2017. Microbes influence the biogeochemical and optical properties of maritime Antarctic snow. *J. Geophys. Res. Biogeosci.* 122, 1456–1470. <https://doi.org/10.1002/2016JG003694>.
- Hoham, R.W., Duval, B., 2001. Microbial ecology of snow and freshwater ice with emphasis on snow algae. In: Jones, H.G., Pomeroy, J.W., Walker, D.A., Hoham, R.W. (Eds.), *Snow Ecology: An Interdisciplinary Examination of Snow-covered Ecosystems*. Cambridge University Press, Cambridge, pp. 168–228.
- Jakob, T., Schreiber, U., Kirchesch, V., Langner, U., Wilhelm, C., 2005. Estimation of chlorophyll content and daily primary production of the major algal groups by means of multiwavelength-excitation PAM chlorophyll fluorometry: performance and methodological limits. *Photosynth. Res.* 83, 343–361.
- Keshava, N., Mustard, J.F., 2002. Spectral unmixing. *IEEE Signal Process. Mag.* 19, 44–57. <https://doi.org/10.1109/79.974727>.
- Kokhanovsky, A., Lamare, M., Mauro, B. Di, Picard, G., Arnaud, L., Dumont, M., Tuzet, F., Brockmann, C., 2018. On the reflectance spectroscopy of snow 1–26. doi:10.5194/10.5194/10.11-26-2018-72.
- Latifovic, R., Olthof, I., 2004. Accuracy assessment using sub-pixel fractional error matrices of global land cover products derived from satellite data. *Remote Sens. Environ.* 90, 153–165.
- Laybourn-Parry, J., Tranter, M., Hodson, A.J., 2013. *The Ecology of Snow and Ice Environments* Oxford. University Press.

- Liang, S., 2001. Narrowband to broadband conversions of land surface albedo I: algorithms. *Remote Sens. Environ.* 76, 213–238. [https://doi.org/10.1016/S0034-4257\(00\)00205-4](https://doi.org/10.1016/S0034-4257(00)00205-4).
- Lutz, S., Anesio, A.M., Villar, J., Benning, L.G., 2014. Variations of algal communities cause darkening of a Greenland glacier. *FEMS Microbiol. Ecol.* 89, 402–414. <https://doi.org/10.1111/1574-6941.12351>.
- Lutz, S., Anesio, A.M., Raiswell, R., Edwards, A., Newton, R.J., Gill, F., Benning, L.G., 2016. The biogeography of red snow microbiomes and their role in melting arctic glaciers. *Nat. Commun.* 7, 11968. <https://doi.org/10.1038/ncomms11968>.
- Musilova, M., Tranter, M., Bamber, J.L., Takeuchi, N., Anesio, A.M., 2016. Experimental evidence that microbial activity lowers the albedo of glaciers. *Geochem. Perspect. Lett.* 2, 106–116. <https://doi.org/10.7185/geochemlet.1611>.
- Na, G., Liu, C., Wang, Z., Ge, L., Ma, X., Yao, Z., 2011. Distribution and characteristics of PAHs in snow of Fildes Peninsula. *J. Environ. Sci.* 23, 1445–1451.
- Naegeli, K., Damm, A., Huss, M., Wulf, H., Schaefer, M., Hoelzle, M., 2017. Cross-comparison of albedo products for glacier surfaces derived from airborne and satellite (Sentinel-2 and Landsat 8) optical data. *Remote Sens.* 9, 1–22. <https://doi.org/10.3390/rs90201010>.
- Oliva, M., Navarro, F., Hrbáček, F., Hernández, A., Nývlt, D., Pereira, P., Ruiz-Fernández, J., Trigo, R., 2017. Recent regional climate cooling on the Antarctic Peninsula and associated impacts on the cryosphere. *Sci. Total Environ.* 580, 210–223. <https://doi.org/10.1016/j.scitotenv.2016.12.030>.
- Painter, T.H., Duval, B., Thomas, W.H., Mendez, M., Heintzelman, S., Dozier, J., 2001. Detection and quantification of snow algae with an airborne imaging spectrometer. *Appl. Environ. Microbiol.* 76, 5267–5272. <https://doi.org/10.1128/AEM.67.11.5267-5272.2001>.
- Roberts, D., Gardner, M., Church, R., Ustin, S., Scheer, G., Green, R., 1998. Mapping chaparral in the Santa Monica Mountains using multiple endmember spectral mixture models. *Remote Sens. Environ.* 65, 267–279.
- Schmid, T., López-Martínez, J., Guillaso, S., Serrano, E., D'Hondt, O., Koch, M., Nieto, A., O'Neill, T., Mink, S., Duránh, J.J., Maestro, A., 2016. Geomorphological mapping of ice-free areas using polarimetric RADARSAT-2 data on Fildes Peninsula and Ardley Island, Antarctica. *Geomorphology* 293, 448–459. <https://doi.org/10.1016/j.geomorph.2016.09.031>.
- Shevnina, E., Kourzeneva, E., 2017. Thermal regime and components of water balance of lakes in Antarctica at the Fildes Peninsula and the Larsemann Hills. *Tellus A* 69 (1), 1317202. <https://doi.org/10.1080/16000870.2017.1317202>.
- Shimada, R., Takeuchi, N., Aoki, T., 2016. Inter-annual and geographical variations in the extent of bare ice and dark ice on the Greenland ice sheet derived from MODIS satellite images. *Front. Earth Sci.* 4, 43. <https://doi.org/10.3389/feart.2016.00043>.
- Shin, J., Kim, H.C., Kim, S., Hong, S.G., 2014. Vegetation abundance on the Barton Peninsula, Antarctica: estimation from high-resolution satellite images. *Polar Biol.* 37, 1579–1588.
- Sibandze, P., Mhangara, P., Odindi, J., Kganyago, M.A., 2014. Comparison of normalised difference snow index (NDSI) and normalized difference principal component snow index (NDPCSI) techniques in distinguishing snow from related land cover types. *South Afric. J. Geomat.* 3, 197–209. <https://doi.org/10.4314/sajg.v3i2.6>.
- Somers, B., Asner, G.P., Tits, L., Coppin, P., 2011. Endmember variability in spectral mixture analysis: a review. *Remote Sens. Environ.* 115, 1603–1616. <https://doi.org/10.1016/j.rse.2011.03.003>.
- Takeuchi, N., Dial, R., Kohshima, S., Segawa, T., Uetake, J., 2006. Spatial distribution and abundance of red snow algae on the Harding Icefield, Alaska derived from a satellite image. *Geophys. Res. Lett.* 33, L21502. <https://doi.org/10.1029/2006GL027819>.
- Tedesco, M., Doherty, S., Warren, W., Tranter, M., Stroeve, J., Fettweis, X., Alexander, P., 2015. What darkens the Greenland ice sheet? *Eos* 96, 2015. <https://doi.org/10.1029/2015EO035773>. Published on 17 September.
- Tedesco, M., Doherty, S., Fettweis, X., Alexander, P., Jeyaratnam, J., Stroeve, J., 2016. The darkening of the Greenland ice sheets: trends, drivers, and projections (1981–2100). *Cryosphere* 10, 477–496. <https://doi.org/10.5194/tc-10-477-2016>.
- Tedstone, A.J., Bamber, J.L., Cook, J.M., Williamson, C.J., Fettweis, X., Hodson, A.J., Tranter, M., 2017. Dark ice dynamics of the south-west Greenland ice sheet. *Cryosphere* 11, 2491–2506. <https://doi.org/10.5194/tc-11-2491-2017>.
- Thomas, W.H., Duval, B., 1995. Sierra Nevada, California, USA, snow algae: snow albedo changes, algal-bacterial interrelationships, and ultraviolet radiation effects. *Arct. Alp. Res.* 27, 389–399.
- Tranter, M., Jones, H.G., 2001. The chemistry of snow: processes and nutrient cycling. In: Jones, H.G., Pomeroy, J.W., Walker, D.A., Hoham, R. (Eds.), *The Ecology of Snow. An Interdisciplinary Examination of Snow-covered Ecosystems*. Cambridge University Press, pp. 127–167.
- Turner, J., Lu, H., White, I., King, J.C., Phillips, T., Scott Hosking, J., Bracegirdle, T.J., Marshall, G.J., Mulvaney, R., Deb, P., 2016. Absence of 21st century warming on Antarctic Peninsula consistent with natural variability. *Nature* 535. <https://doi.org/10.1038/nature18645>.
- Vaughan, D.G., Doake, C.S.M., 1996. Recent atmospheric warming and retreat of ice shelves on the Antarctic Peninsula. *Nature* 379, 328–331.
- Vaughan, D.G., Marshall, G.J., Connolley, King, J.C., Mulvaney, R., 2001. Devil in the detail. *Science* 293, 1777–1779.
- Vaughan, D.G., Marshall, G.J., Connolley, W.M., Parkinson, C., Mulvaney, R., Hodgson, D.A., King, J.C., Pudsey, C.J., Turner, J., 2003. Recent rapid regional climate warming on the Antarctic Peninsula. *Clim. Change* 60, 243–274.
- Vieira, G., Mora, C., Pina, P., Schaefer, C.E.R., 2014. A proxy for snow cover and winter ground surface cooling: Mapping *Usnea* sp. communities using high resolution remote sensing imagery (Maritime Antarctica). *Geomorphology* 225, 69–75.
- Vogt, S., Braun, M., 2004. Influence of glaciers and snow cover on terrestrial and marine ecosystems as revealed by remotely-sensed data. *Revista de Pesquisa Antartica Brasileira* 4, 105–118.
- Wiscombe, W.J., Warren, S.G., 1980. A Model for the spectral albedo of snow. I: pure snow. *J. Atm. Sci.* 37, 2712–2733.
- Warren, S.G., Wiscombe, W.J., 1980. A Model for the spectral albedo of snow. II: snow containing atmospheric aerosols. *J. Atm. Sci.* 37, 2734–2745.
- Yallop, M.L., Anesio, A.M., Perkins, R.G., Cook, J., Telling, J., Fagan, D., MacFarlane, J., Stibal, M., Barker, G., Bellas, C., Hodson, A., Tranter, M., Wadham, J., Roberts, N.W., 2012. Photophysiology and albedo-changing potential of the ice algal community on the surface of the Greenland ice sheet. *ISME J.* 6, 2302–2313. <https://doi.org/10.1038/ismej.2012.107>.